Response of East Asian climate to Dansgaard/Oeschger and Heinrich events in a coupled model of intermediate complexity

Liya Jin,[1] Fahu Chen,[1] Andrey Ganopolski,[2] and Martin Claussen[3]

Received 19 March 2006; revised 4 October 2006; accepted 1 November 2006; published 29 March 2007.

[1] Terrestrial records of loess-paleosol sequences from across the Asian interior (Chinese Loess Plateau) have been used to reconstruct climatic conditions through the Quaternary and they correlate, in general, with oxygen isotope records from deep sea cores (e.g., the grain-size maxima from Chinese loess with ages that match well those of the last six Heinrich events evidenced in the North Atlantic marine sediments during the last glacial period). Possible reasons for this teleconnection of the similar climate signal of the North Atlantic and China are investigated by using an Earth system model of intermediate complexity (CLIMBER-2) for the typical period of last glacial age (during 60–20 kyr BP). By using the CLIMBER-2 model, we have studied the response of East Asian climate during the typical glacial age (60–20 kyr BP) to Dansgaard/Oeschger (D/O) and Heinrich events. To trigger D/O and Heinrich events in the model, transient forcings in addition to changes in insolation caused by variations in the Earth orbit are prescribed in the modeling experiment. These additional forcings include changes in inland-ice volume over North America, in freshwater flux into the northern North Atlantic. The modeling results show that the variations of the annual-mean near-surface air temperature over Eurasia closely follow climate changes in North Atlantic. The stronger intensity of westerly wind in the midlatitude of northern hemisphere versus the weaker Asian summer monsoon as well as the slightly weaker Asian winter monsoon (north easterly flow near surface) corresponds well with the (prescribed) Heinrich events during 60–20 kyr BP. This suggests that the climate signals found in Chinese loess (grain-size maxima with ages that match those of the last six Heinrich events) during the last glaciation are likely related to the relatively stronger westerly winds over Eurasia in boreal winter and a relatively weaker Asian summer monsoon that intensified the aridity of northern China which lead to expansion of the northern deserts during the Heinrich events.

Citation: Jin, L., F. Chen, A. Ganopolski, and M. Claussen (2007), Response of East Asian climate to Dansgaard/Oeschger and Heinrich events in a coupled model of intermediate complexity, *J. Geophys. Res.*, *112*, D06117, doi:10.1029/2006JD007316.

1. Introduction

[2] The study of paleoclimatic records has revealed that climate was highly variable during glacial times [*Dansgaard et al.*, 1993]. Two of the best-known and best-documented types of abrupt and strong shifts in glacial climate were found in Greenland ice cores and North Atlantic marine sediments, termed as Dansgaard-Oeschger (D/O) [*Dansgaard et al.*, 1982; *Grootes et al.*, 1993] and Heinrich events [*Heinrich*, 1988; *Bond et al.*, 1992]. The D/O events are characterized by an abrupt warming of up to 10°C in Greenland and North Atlantic region within a few years or 1 decade. The abrupt warming is followed by a gradual cooling over several hundred or thousand years and a relative rapid drop of temperatures to stadial values. Heinrich events are associated with episodes of massive iceberg discharges into the North Atlantic Ocean from the surrounding ice sheets [*Broecker et al.*, 1992] and occurred irregularly with a typical recurring time of around 7000 years. Geological data suggest that the region surrounding Hudson Bay was the major source of icebergs for most Heinrich events. Sediments also indicate that Heinrich events drastically reduce, or even shut down, the formation of North Atlantic Deep Water [*Elliot et al.*, 2002]. In most cases, Heinrich events are followed by a particularly warm D/O event, and successive D/O events tend to become progressively cooler until the next Heinrich event starts.

[3] Although the strongest D/O and Heinrich events are recorded in data for Greenland and the Northern Atlantic, many of the similar climate signals of D/O events and Heinrich events have also been reported outside the North Atlantic region all over the world, as indicated by several terrestrial climate records [*Grimm et al.*, 1993; *Guiot et al.*,

[1] Key Laboratory of Western China's Environmental Systems (Ministry of Education) and Key Laboratory of Arid Climatic Changing and Reducing Disaster of Gansu Province, Lanzhou University, Lanzhou, China.
[2] Potsdam Institute for Climate Impact Research, Potsdam, Germany.
[3] Meteorological Institute, University Hamburg and Max Planck Institute for Meteorology, Hamburg, Germany.

0148-0227/07/2006JD007316

1993; *Broecker*, 1994; *Lowell et al.*, 1995; *Voelker and workshop participants*, 2002]. There are increasing evidences that the millennial-scale climate variability reconstructed in many climate proxies is related in some way to the D/O and Heinrich events. In the Asian region, some of the evidences have been identified in the extensive Loess Plateau of central China (see Figure 1 and Figure 3 for position of the Chinese Loess Plateau), where alternating loess and paleosol sequences derived from loess sections provide an excellent long-term proxy record of climate change [e.g., *Liu*, 1985; *Kukla and An*, 1989; *Ding et al.*, 1992, 1994; *Verosub et al.*, 1993]. A correlation between Chinese loess records based on grain-size date from Luochuan loess section and the Heinrich events has been proposed by *Porter and An* [1995], which shows that grain-size maxima with ages match well those of the last six Heinrich events. According to the model assumptions to reconstruct the grain-size chronology, the coarse-grain-size maxima in the loess-paleosol record are inferred to mark times when the competency and capacity of dust-bearing winds increased [*Porter and An*, 1995], and hence the grain-size maxima are commonly interpreted as an indication of the changing strength of the East Asian winter monsoon [*Xiao et al.*, 1995]. There are more other documents from loess-paleosol sequences of last glacial periods showing that a series of colder and/or drier events can be temporally correlated with the North Atlantic Heinrich events [e.g., *Guo et al.*, 1996; *Ren et al.*, 1996; *Ding et al.*, 1999; *Porter*, 2001]. In addition to the research on the Chinese loess-paleosol sequences, there are many other proxy data recorded abrupt changes in East Asia that are related to Heinrich events. The high-resolution record of variations in planktonic foraminiferal oxygen isotopes (δ^{18}O) from the IMAGES MD97-2141 core (8.80°N, 121.31°E) in the Sulu Sea located in the Philippine archipelago of western tropical Pacific show important rapid oscillations which appear synchronous with some Heinrich events [*Linsley*, 1996]. The δ^{18}O records of five stalagmites from Hulu Cave in eastern China, which can be representative of the East Asian summer monsoon intensity, bear a remarkable resemblance to that from Greenland ice cores [*Wang et al.*, 2001]. For the D/O oscillations recorded in ice cores, the Chinese loess-paleosol record exhibits also comparable shifts [*Chen et al.* 1997]. The primary productivity (PP) sequence reconstructed from coccoliths in the IMAGES MD97-2141 core (8.80°N, 121.31°E), which is used as indication of East Asian winter monsoon variations, has frequencies near those of the D/O cycles in North Atlantic ice records [*de Garidel-Thoron et al.*, 2001].

[4] As the location of Chinese loess deposits and other proxy data in East Asia are remote from the North Atlantic region, the causes responsible for such similar climate events in China and in East Asia or the link of the climates between the North Atlantic and East Asia (including China) are not yet fully understood. The paleomonsoon theory has been used to interpret the loess-paleosol sequences as the products of Asian monsoon circulation [*An et al.*, 1991a, 1991b]. Grain size changes of loess records are generally interpreted as having been controlled by changes in wind intensity, and grain size was used as a proxy of Asian winter monsoonal changes [*An et al.*, 1991c; *Ding et al.*, 1992]. However, further studies on loess records show that changes in the sand particle content of the loess deposits seem to be controlled firstly by changes in the position of the desert, and grain size changes of loess deposits are related to the extent of dust source regions, wind intensity as well as postdepositional weathering [*Ding et al.*, 1999]. Paleodesert studies have shown that during the glacial-interglacial cycles, the deserts in northern China have experienced a large-scale change in position [*Dong et al.*, 1990]. So the increase in grain size in the loess cannot be solely attributed to the increase in wind strength; in other words, it seems that loess particles in the Chinese Loess Plateau reaching a maximum value during Heinrich events may not be simply interpreted by an increase in the Asian winter monsoon, and the advance-retreat changes of the deserts in northern China may be the most important factor controlling changes in the sand particle percentage of the loess-paleosol sequence [*Ding et al.*, 1999].

[5] There are also reports of the Asian summer monsoonal changes in conjunction with the Heinrich events. Studies on sections in the Chinese Loess Plateau show that paleoweathering indices of loess can be used as sensitive indicators of plaeoclimatic changes, in which the high weathering intensity can be interpreted as an indication of strengthened summer monsoon, while lower weathering intensity indicates the reverse [*Guo et al.*, 1996]. A series of colder and/or drier events, as indicated by the lower values of the weathering indices, corresponding to a significant weakening of the Asian summer monsoon, have been documented in the loess of the last glacial periods, which can be temporally correlated with the North Atlantic Heinrich events [*Guo et al.*, 1996]. Other quantitative estimates of climates based on pollen records which have been reported from the African monsoon zone [*Bonnefille et al.*, 1992; *Vincens et al.*, 1993] and from the South China Sea (Zhujiang-Q4 Core, 22°22′N, 115°25′E) [*Lü et al.*, 1991] show significant cooling events around 14, 21, and 27 ^{14}C-kyr BP [*Bonnefille et al.*, 1992; *Vincens et al.*, 1993] as well as at ~13.9–~14.7 ky BP and ~20.6–~22.9 kyr BP, respectively, temporally correlative with the lower weathering intensity intervals of Chinese Loess Plateau [*Guo et al.*, 1996]. Thus the general cooling (or/and drying) in the African-Asian monsoon zone seems to indicate that the Asian summer monsoon have also experienced high-frequency changes (weakened summer monsoon) approximately synchronous with the Heinrich events.

[6] It is also thought that the Chinese loess grain-size variations (which are considered associated with the Asian winter monsoon regime) may have been linked with the Heinrich events through the westerlies [*Porter and An*, 1995]. The link between Chinese loess and the North Atlantic basin is established by transport of dust of Asian origin via what was probably a northern branch of the jet stream to Greenland and the Greenland Ice Sheet Project Two (GISP2) ice-core [*Biscaye et al.*, 1997]. Previous climate-model simulations of full-glacial conditions are consistent with such an inference that in glacial conditions, atmospheric circulation was enhanced and surface storm tracks had a latitudinal displacement; these tracks passed to the south of the North American ice sheets and then across the North Atlantic ice-rafted detritus (IRD) zone, southern Europe, and central Asia toward the Loess Plateau [*Kutzbach et al.*, 1993; *Manabe and Stouffer*, 1988]. Thus

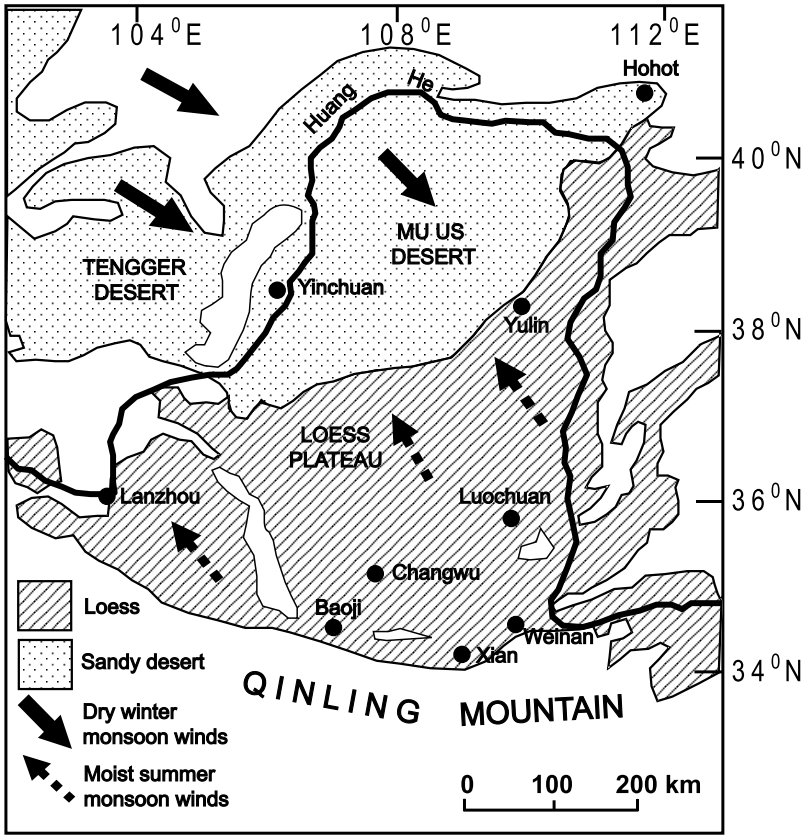

Figure 1. Map of the Chinese Loess Plateau, position of northern deserts, the East Asian summer, and winter monsoon circulations (after *Guo et al.* [2000]).

the effect of westerly wind is probably an important influential factor for a transcontinental teleconnection. However, sedimentary dynamic illustration also indicates that the coarse component of grain-size of the Chinese loess was mostly the product of lower-atmospheric winter monsoonal winds, and the fine component was mainly transported in upper atmospheric circulation dominated by westerly in northern China [*Sun et al.*, 2003].

[7] Although abundant proxy records from East Asia have revealed the presence of both Heinrich events and D/O cycles in the last glacial period as have been summarized above, the mechanism that the climatic signals were transferred from North Atlantic into the East Asian monsoon system is still not fully clear. Here we summarize the main proposed possible mechanisms that are concerned with (1) the high-frequency changes of Asian winter monsoon, (2) the westerly changes in Northern Hemisphere, and (3) more arid conditions due to weaker Asian summer monsoon, as well as (4) a mix of two or three of above ones. To have a better understanding of the response of East Asian climate to the Heinrich events and D/O cycles as well as of the possible mechanism for a transcontinental teleconnection between the North Atlantic climate variability and the Chinese loess record during the last glacial period, a coupled global model of intermediate complexity herein is employed. After describing model and experimental design in section 2, section 3 is devoted to simulation results, with emphasis on Asian monsoon domain. The study is briefly discussed and concluded in section 4.

2. Model and Experiment Setup

2.1. Model

[8] For the experiments presented here we used an Earth system model of intermediate complexity CLIMBER-2, which is described in detail in the works of *Petoukhov et al.* [2000] and *Ganopolski et al.* [2001]. CLIMBER-2 has a coarse resolution of 10 degrees in latitude and approximately 51° in longitude in the atmosphere. The model of the atmosphere is based on the statistical-dynamical approach and explicitly resolves the large-scale circulation patterns: subtropical jet streams, Hadley, Ferrel and polar cells, monsoon and Walker circulations, tropospheric quasi-stationary planetary waves, and centers of action such as the Siberian high-pressure area and the Aleutian low-pressure area. It does not resolve individual synoptic weather systems but rather predicts their statistical characteristics, including the fluxes of heat, moisture, and momentum associated with ensembles of synoptic systems. The vertical structure includes a planetary boundary layer, a free troposphere (including cumulus and stratiform clouds) and a stratosphere. Radiative fluxes are computed on 16 vetical levels. The ocean model is a multibasin, zonally averaged model similar to the one used by *Stocker et al.* [1992], including a model of sea-ice thickness, concentration, and

advection. The model of terrestrial vegetation [*Brovkin et al.*, 2002] predicts the dynamics of vegetation structure, i.e., fractional coverage of a grid cell by trees, grass, and desert, as well as net primary productivity, leaf area index, biomass, and soil carbon pools.

[9] The CLIMBER-2 model has realistically reproduced the large-scale pattern in present-day climate [*Petoukhov et al.*, 2000] and has successfully been applied to paleoclimatic simulations of the last glacial maximum [*Ganopolski et al.*, 1998] and changes in the global carbon cycle [*Brovkin et al.*, 2002]. CLIMBER-2 also reproduces the characteristic time evolution of D/O events and Heinrich events, the recovery of North Atlantic Deep Water (NADW) formation after Heinrich events, etc. [*Ganopolski and Rahmstorf*, 2001a, 2001b, 2002]. CLIMBER-2 has also been used in a series of sensitivity experiments [e.g., *Jin et al.*, 2005].

2.2. Experiment Setup

[10] To simulate the climate variations of the time interval from 60 kyr BP to 20 kyr BP, we have to prescribe changes in the boundary conditions that are external to the climate system (i.e., insolation) or internal. The internal boundary conditions concern the heat, momentum and mass fluxes at the interface between components of the climate system that are explicitly simulated by the model. In this study the dynamics of the atmosphere, ocean, and land surface/vegetation are simulated explicitly while the motion of inland ice and resulting freshwater fluxes are prescribed.

[11] In the experiments, insolation was varied by changes in orbital parameters [*Berger*, 1978]. Submillennial variations in solar energy flux were not taken into account, and the atmospheric CO_2 concentration was kept constant at 200 ppm. Hence we neglected the effect of small variations atmospheric CO_2 of approximately 20–30 ppm reconstructed for stadial-interstadial changes [e.g., *Petit et al.*, 1999].

[12] To simulate abrupt climate changes, we added a freshwater forcing, which consists of three components. All three components were applied to the North Atlantic between 50°N and 70°N with the maximum amplitude at 60°N. The first component is associated with the hydrological impact of Heinrich events, and it represents regular pulses of freshwater with the amplitude of 0.15 Sv (1 Sv = 10^6 m^3 s^{-1}) and a period of 7500 years. Such pulses cause a temporal complete shutdown of the thermohaline circulation (THC) [*Ganopolski and Rahmstorf*, 2001a, 2001b]. Second, to trigger D/O events, we introduced a white-noise freshwater anomaly. This component represents the ubiquitous internal variability of the atmosphere–ocean system that is not explicitly simulated in our model. The standard deviation of the freshwater anomaly was 0.035 Sv. The white-noise freshwater flux is strong enough to trigger randomly varying D/O events. Third, the D/O events were synchronized by a small freshwater forcing of 0.01 Sv and a period of 1500 years. The small forcing is too weak to generate D/O events by itself. It just synchronizes D/O events via the mechanism of stochastic resonance [*Ganopolski and Rahmstorf*, 2002]. The latter freshwater forcing, unlike the previous freshwater forcings, is hypothetic, and its origin is unknown so far. Inclusion of such forcing allows to reproduce several important features of the D/O events known from paleodata [*Alley et al.*, 2001].

[13] The inland ice dynamics including ice surges from the Laurentide ice sheet with amplitudes and periodicity of freshwater pulses mentioned above have been simulated by *Calov et al.* [2002]. Here, we just applied gradual variations of the thickness and area of Laurentide and Fennoscandian ice sheets, although rather schematic, but nevertheless consistent with paleoreconstructions and global sea level variations during 60–20 kyr BP. In the case of Heinrich events, the volume of inland ice sheets was varied consistently with the imposed freshwater anomaly. The change in ice mass during a Heinrich event thus led to a change in sea level of some 10 m. The reduction of the thickness of Laurentide ice sheet was, accordingly, 750 m in the latitudinal belt between 40°N and 60°N. The set of external forcings of the numerical experiments for simulation of the last glacial cycle (the time interval from 60 kyr BP to 20 kyr BP) are shown in Figures 2a and 2b.

3. Model Results

3.1. Present-Day Climate for Sea Level Pressure (SLP) and Surface Winds in CLIMBER-2

[14] The performance of the fully coupled climate model, the CLIMBER-2, for modern climate conditions, have been presented in detail by *Petoukhov et al.* [2000] and by *Ganopolski et al.* [2001]. Here we only give the simulated global spatial distribution of SLP and surface winds (shown in Figure 3) to demonstrate the ability of the model for simulation of the present-day climate, which is a basis for using the model to study climates in the past. "Modern" means hereafter the present-day Earth geography, solar insolation, and preindustrial CO_2 concentration (280 ppm). The distribution of potential vegetation was prescribed. To reach the equilibrium climate state, the coupled model was integrated for 5000 years.

[15] Figures 3a and 3b shows the simulated present-day global pattern of winter and summer sea level pressure (SLP) and composite near-surface wind, in which the modeling results by and large agree with observational data [e.g., *Peixoto and Oort*, 1992] in respect of the large-scale patterns of SLP for both seasons, including positions and absolute values of the stationary high (e.g., the Siberian high pressure cell in boreal winter) and low-pressure (e.g., the Asian low pressure cell in boreal summer) systems in the subtropics and midlatitudes. The seasonally alternating circulation of the East Asian monsoon system from winter to summer is clearly simulated, which shows that the model is able to simulate present-day climate and its variability in East Asia fairly realistically. In the following sections, we will analyze the simulated results for the last glacial period during 60–20 kyr BP.

3.2. Near-Surface Air Temperature Over Eurasian Continent During 60–20 kyr BP

[16] As it was shown in earlier studies [*Ganopolski and Rahmstorf*, 2001a, 2001b; *Claussen et al.*, 2003] under glacial climate conditions, the Atlantic thermohaline circulation becomes relatively unstable, which results in abrupt transitions between two modes ("cold" and "warm"; see the works of *Ganopolski and Rahmstorf* [2001a, 2001b]) of

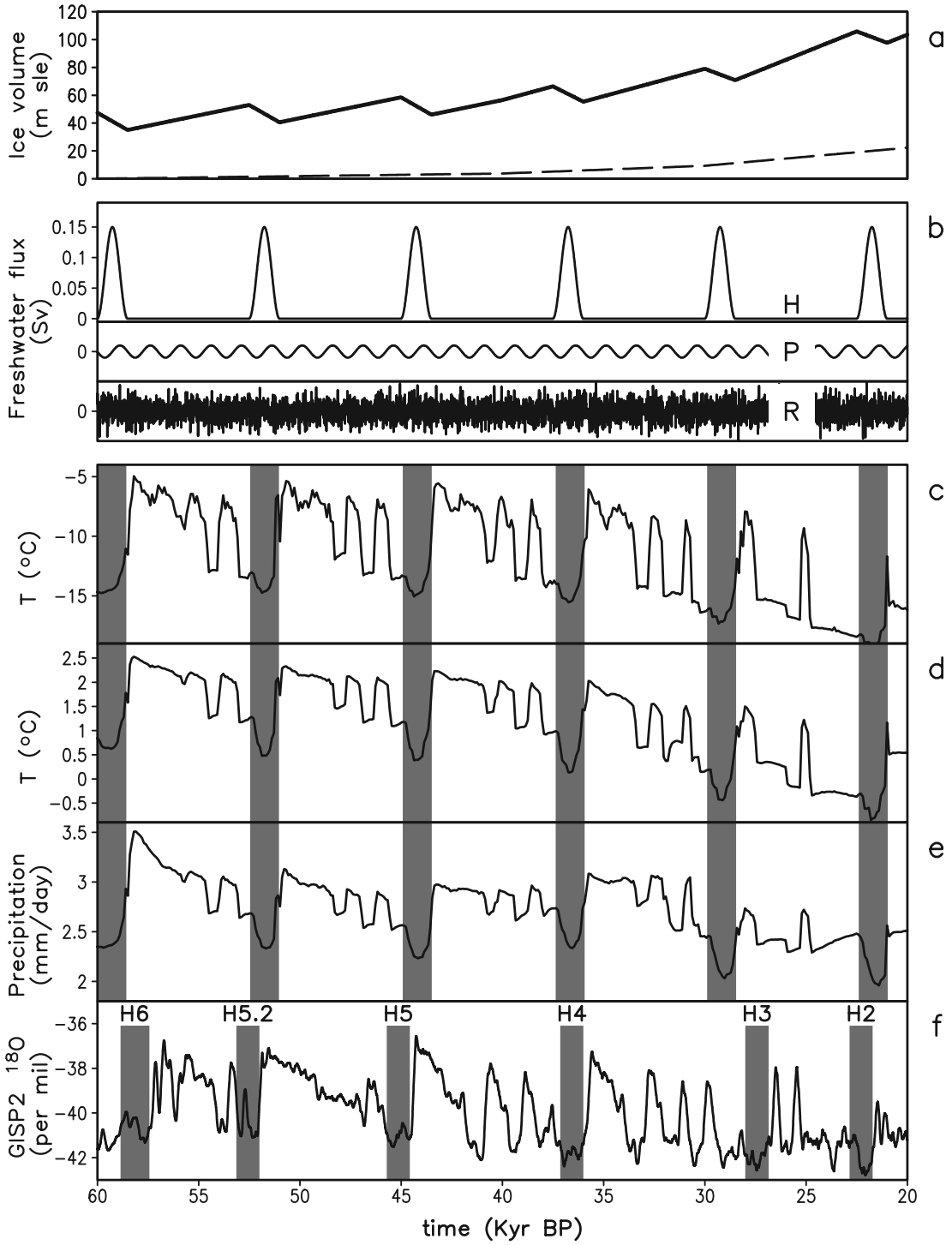

Figure 2. Transient forcings of the numerical experiments for simulation of the last glacial cycle (the time interval from 60 kyr BP to 20 kyr BP). (a) Prescribed evolution of inland-ice volume, given in meters of sea-level change (m SL). Solid line indicates ice volume of Laurentide, and dashed line, Eurasian ice volume. (b) Freshwater forcing applied in the North Atlantic, given in Sverdrup (1 Sv = 10^6 m^3 s^{-1}). The upper line (H) indicates the freshwater forcing to trigger Heinrich events, i.e., meltwater pulses with a period of 7500 years and an amplitude of 0.15 Sv. The lowest curve (R) is random forcing at high northern latitudes which triggers D/O events. The middle curve (P) is a sinusoidal forcing which itself is too weak to trigger D/O events, but which is able to synchronize D/O events via the mechanism of stochastic resonance. Simulated time series of (c) annual surface air temperature in the North Atlantic (around 60°N–70°N, 65°W–15°W), (d) over Eurasian continent (around 40°N–50°N, 40°E–90°E), and (e) summer precipitation in East Asia (around 20°N–30°N, 90°E–140°E), and (f) Oxygen isotope of GISP2. Shading areas for the data corresponding the timing of freshwater forcing and Heinrich events.

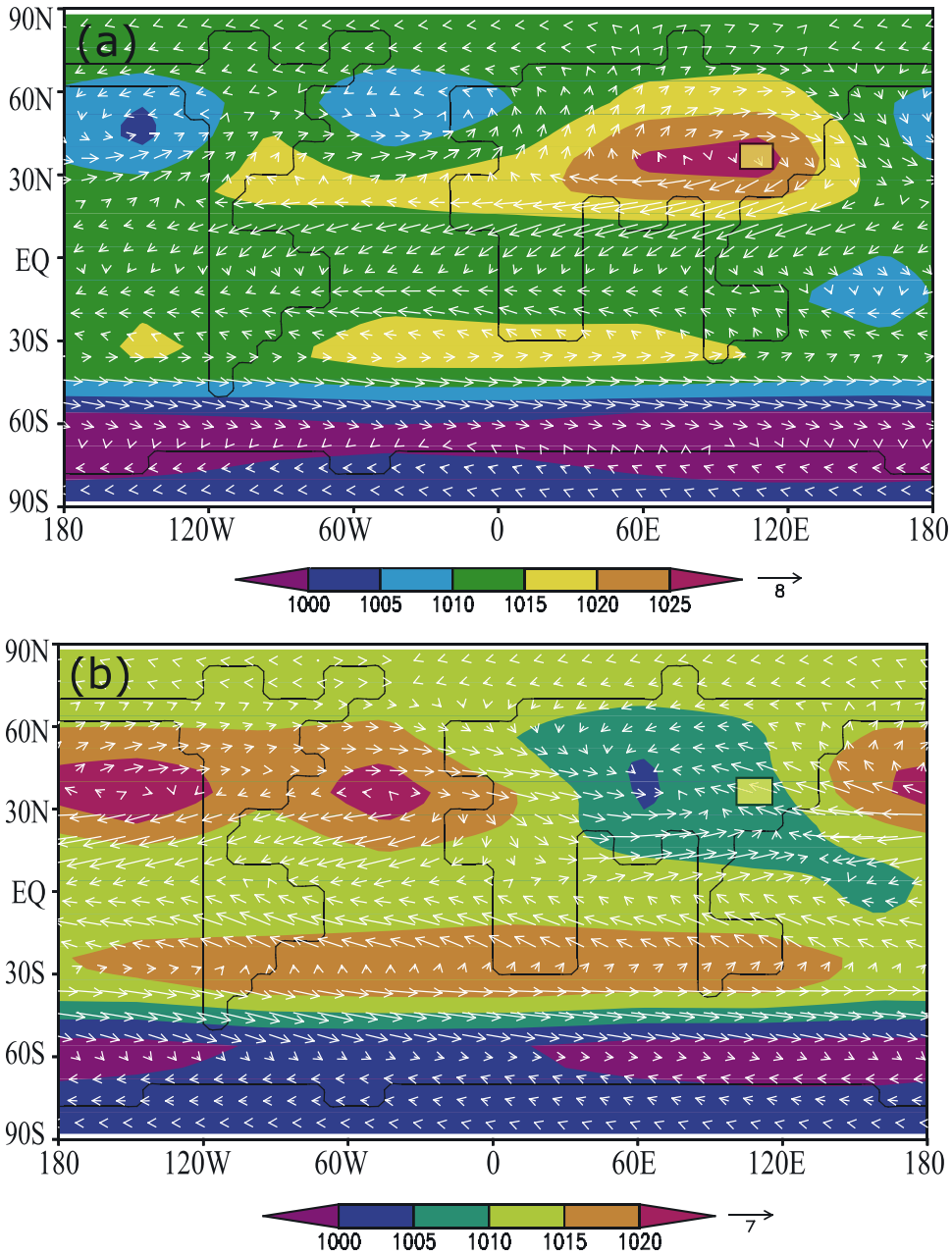

Figure 3. Simulated present-day global pattern of winter (a) and summer (b) sea level pressure (SLP) (unit: hPa) and corresponding mean near-surface wind (unit: m/s). The wind shown here (and in Figure 6) is plotted by using a spatial bi-lineal interpolation. The yellow square in this figure (and in Figure 6 and Figure 7) corresponds to the area in Figure 1.

the Atlantic circulations under a small variation of surface freshwater flux. These changes in the oceanic circulations leads to strong variations of the poleward flux in the northern North Atlantic, which, being amplified by sea ice feedback, leads to abrupt changes in the atmospheric temperature by about 10°C (Figure 2c). The latter is in a reasonable agreement with empirical estimate of temperature changes in Greenland during several D/O events (10°–15°C) [e.g., *Landais et al.*, 2005]. During Heinrich events, a large freshwater flux into the North Atlantic completely suppressed the thermohaline circulations, but the model does not simulate additional substantial cooling associated with Heinrich events (Figure 2c) which are in agreement with Greenland records [e.g. *Grootes et al.*, 1993] (Figure 2f).

[17] The temperature changes associated with the reorganizations of the Atlantic circulation is not restricted to the North Atlantic realm and via atmospheric circulations a number of atmospheric teleconnections spread over a large part of the globe. In previous works [*Ganopolski and Rahmstorf*, 2001a, 2001b; *Claussen et al.*, 2003] the main attention was given to the Atlantic responses and the mechanism of interhemispheric seesaw. Here we will analyze the

Table 1. Definition of Several Indexes

Index	Definition
u-component	Mean zonal near-surface wind velocity over Eurasia (around 35°N–55°N, 50°E–140°E)
ZI (zonal index)	Horizontal differences of sea level pressure (SLP) between 35°N and 55°N over Eurasia or ZI = $SLP_{35°N}$-$SLP_{55°N}$ during boreal winter (DJF)
AWMI (Asian winter monsoon index)	Average of $-v$ with $v < 0$ over the region of East Asian coast (between 20°N and 30°N, centered at 120°E) and v is the mean meridional surface wind during boreal winter (DJF)
PI (Siberian high pressure intensity)	Sea level pressure averaged over Eurasia (around 35°N–55°N, 50°E–140°E) during boreal winter (DJF)

impact of the Atlantic changes on East Asian climate during glacial age.

[18] The results of the transient simulation during the time interval from 60 kyr BP to 20 kyr BP revealed a pronounced response of CLIMBER-2 to the imposed forcing of perturbations at high northern latitudes. The simulated time series of annual-mean near-surface air temperature over Eurasian continent (around 40°N–50°N, 40°E–90°E) are shown in Figure 2d, which shows a quite similar temperature variation but smaller amplitudes with that in the North Atlantic during 60–20 kyr BP. The similarity of temperature variation between the Eurasian continent and the North Atlantic was tested by a former work conducted by *Claussen et al.* [2003], who calculated the correlation between the time series of near-surface temperature at the grid cell centered at around (65°N, 30°W) (represents the North Atlantic) and that of all atmospheric grid points of CLIMBER-2. Their result shows that at zero time lag between temperature series, the global pattern of correlation reveals positive correlation coefficient of $r > 0.8$ over the North Atlantic and Eurasia (for further details, see *Claussen et al.* [2003, Figure 4a]). The model result of high-temperature correlation between the North Atlantic and Eurasia can be compared with paleoclimatological evidence seen in the North Atlantic marine and ice-core records and in the Chinese loess deposition of central Asian Aeolian dust [*Porter and An*, 1995; *Chen et al.*, 1997], which imply that the climates of the North Atlantic and China were linked in some way, e.g., the effect of westerly winds [*Porter and An*, 1995]. Earlier studies suggest that cold North Atlantic sea surface temperatures could have had a dramatic effect on regions directly downwind in Europe during the last glaciation and the late-glacial Younger Dryas interval [*Guiot et al.*, 1989; *Rind et al.*, 1986]. The temperature variation over the Eurasian continent simulated by CLIMBER-2 indicates that still farther downwind it may be influenced by the climate change in North Atlantic. Recently, *Denton et al.* [2005] pointed out that there was an extreme winter threshold during much of the last glaciation when winter climate crossed this threshold repeatedly, with marked changes in seasonality that may well have amplified and propagated a signal of abrupt change throughout a huge continent sector of the Northern Hemisphere, stretching from Greenland to Asia and into the tropics. In next section, we will analyze the influence of changes in westerlies, East Asian monsoon and the associated aspects on East Asian climate change.

3.3. Westerly Winds, Siberian High Pressure Cell, and East Asian Monsoon

[19] Westerly winds in the planetary circulation system in middle latitudes can be viewed as a link between the climates of the North Atlantic and East Asian area. The East Asian monsoon circulation is mainly located in the lower troposphere system below the long-wave westerly winds near the tropopause [*Chen et al.*, 1991]. The most prominent surface feature of the Asian winter monsoon (AWM) is the strong northeasterly flow (NE) along the eastern flank of the Siberian high and the east coast of the Eurasian continent. The strong NE, starting from the front edge of the Siberian high, periodically pushes toward lower latitudes to become a winter monsoon surge and dominates a vast area of the tropical and extratropical regions of Asia and the western Pacific for nearly half a year [*Chen et al.*, 1991]. As one of the most active and powerful circulations in boreal winter, the AWM variation is closely related with the land-ocean contrast near ground, and the locations and intensities of the east Asian trough and jet stream in the middle and upper troposphere, and cohered with variation of the Hadley cell over the Asian and western Pacific region [*Chen et al.*, 1991]. The East Asian summer monsoon originating from the South and East China Seas is one of the most important climate features over East Asia during northern summer and it contributes most of the annual precipitation for the Loess Plateau. In order to analyze the simulated results of westerly winds, we use the zonal index (ZI) to measure the strength of westerly winds, which is traditionally defined by horizontal sea level pressure (SLP) differences between 35°N and 55°N latitude [*Rossby*, 1939]. And we use the average of $-v$ with $v < 0$ over the region of East Asian coast (around 20°N–30°N, 90°E–140°E) as the Asian winter monsoon index (AWMI) to describe the intensity of the AWM, and v is the mean meridional surface wind in boreal winter (December, January, February, or DJF). The definition of AWMI is similar to that given by *Ji et al.* [1997], *Chen et al.* [1999], and *Hu et al.* [2000]. Since the AWM is closely related to the Siberian High pressure cell, we also define the Siberian High pressure intensity (PI), which is measured by the mean sea level pressure averaged over Eurasian continent (around 35°N–55°N, 50°E–140°E). The definition of the indexes mentioned above is summarized in Table 1.

[20] The simulated time series of ZI, u-component, AWMI, and PI during the period of 60 kyr BP to 20 kyr BP are shown in Figure 4. It is evident that the high phase of ZI (the changing strength of the westerly winds) (Figure 4c) and u-component (Figure 4d) match well to the low phase of AWMI (Figure 4e) and PI (Figure 4f) during 60–20 kyr BP, which correspond to the low phase of annual surface air temperature in the North Atlantic (Heinrich events) (Figure 2c) and over the Eurasian continent (Figure 2d). Our modeling results show that westerlies in boreal winter gradually increased during the last glacial period (60–20 kyr BP), especially during the Heinrich events the

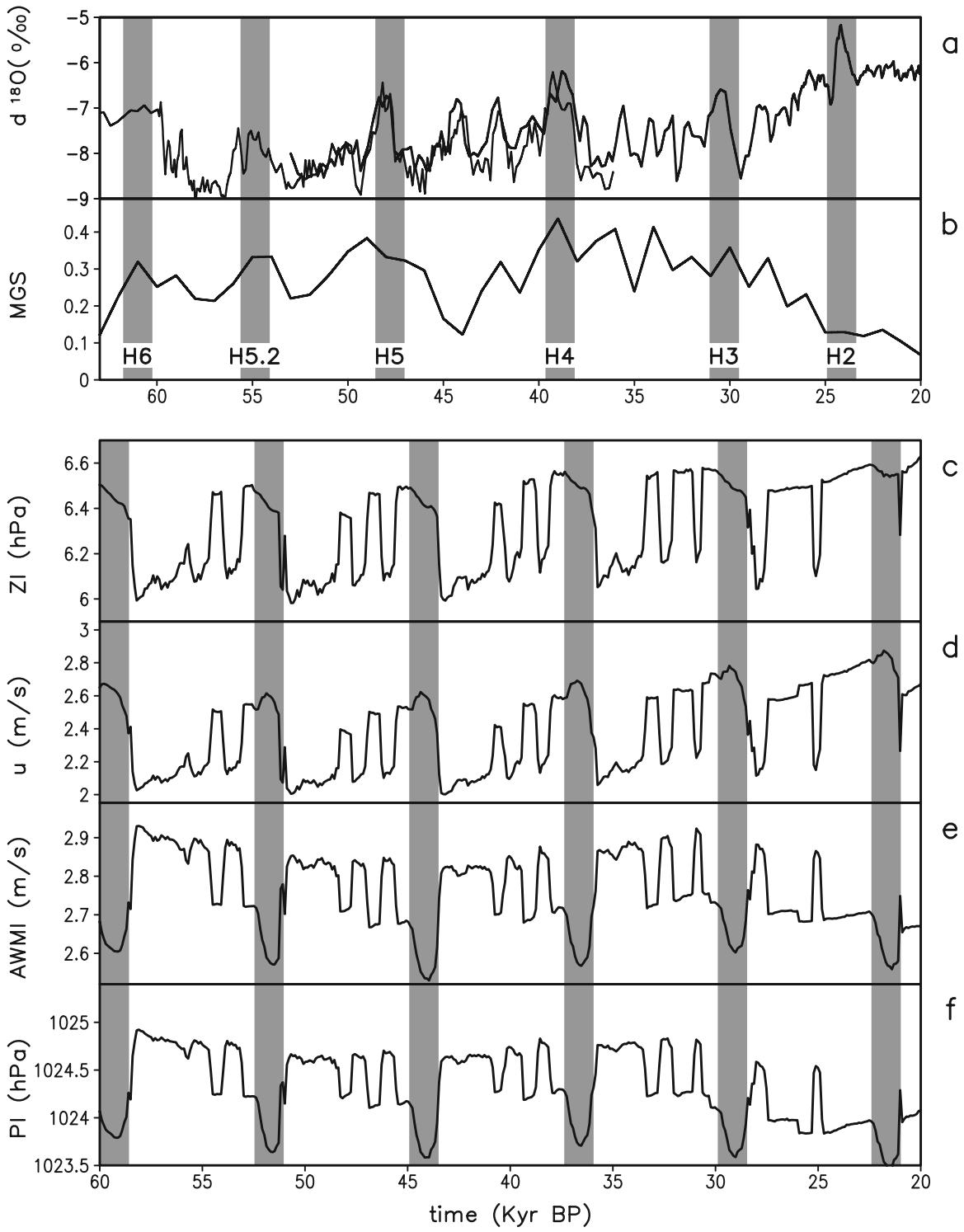

Figure 4. Time series of $\delta^{18}O$ of Hulu Cave stalagmites [*Wang et al.*, 2001] (a), which is as an indicator of East Asian summer monsoon intensity, and Chinese Loess Plateau stacked mean grain size [*Sun et al.*, 2006] (b), as well as simulated time series of (c) westerly index (ZI), (d) u-component over Eurasia continent, (e) the East Asian winter monsoon index (AWMI), and (f) the Siberian High pressure cell index (PI) in boreal winter, representing middle-high latitude westerly winds, the strength of East Asian winter monsoon (northeasterly winds) at east Asian coast (20°N–30°N, centered at 120°E) and the strength of Siberian High in boreal winter respectively. Shading areas for the data in Figures 4a and 4b corresponding the timing of Heinrich events (also included disputed Heinrich event 5.2), while for model results (Figures 4c–4f) the same meanings as in Figure 2.

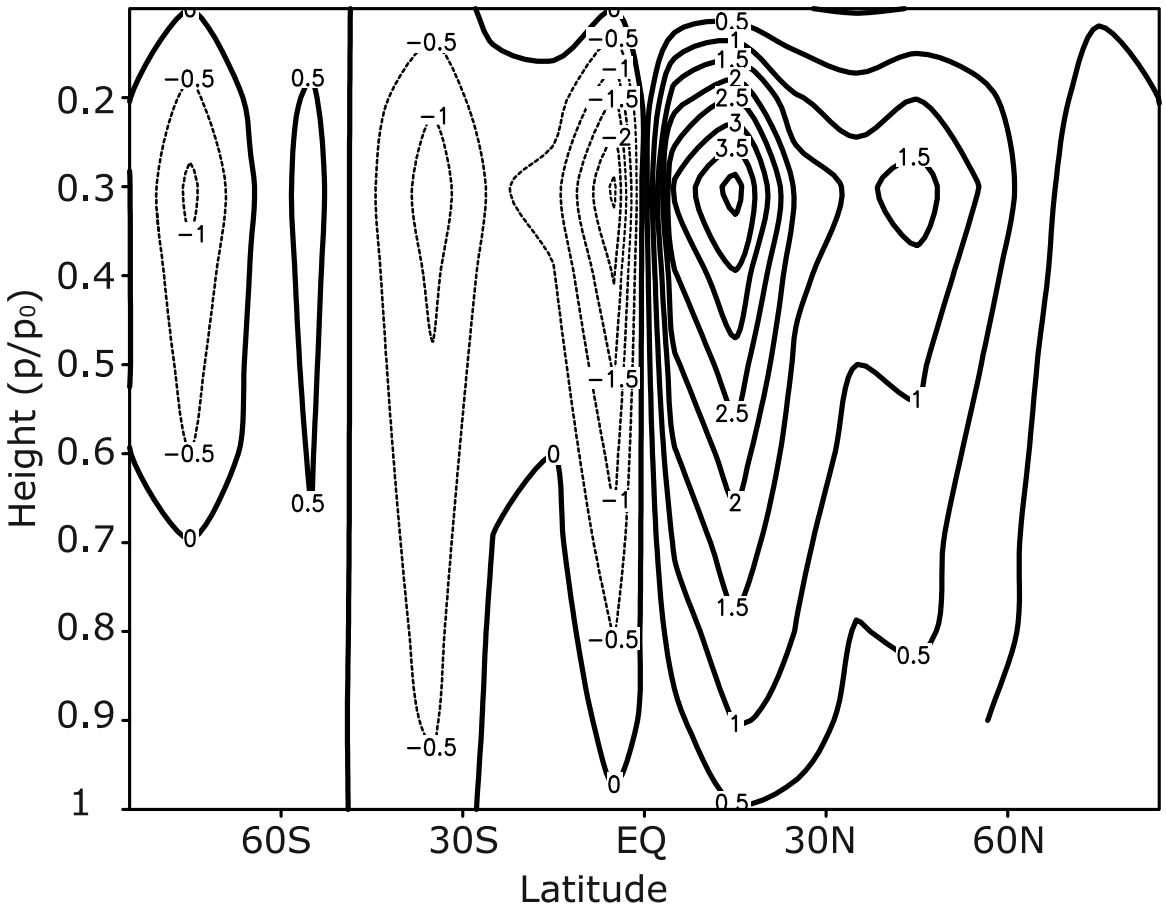

Figure 5. Simulated difference of u-component in a height-latitude section profile, in which the value is the mean value of u-component between 50°E and 140°E (Eurasia) for different latitude from 90°S to 90°N in condition during a Heinrich event minus the warmest phase of a D/O cycle in northern winter (Units are m/s, positive value represents westerly wind, or eastward wind).

westerlies reach maximum (Figures 4c and 4d) while the AWM and Siberian High pressure cell were relatively weaker (Figures 4e and 4f). After that (a Heinrich event) the westerlies decrease abruptly corresponding to the rapid warming (rapidly increased temperature in Figure 2c) between the Heinrich events (cold phase) and the D/O events (warm phase). Because we have prescribed an arbitrary forcing the time series shown in Figures 2c–2d and in Figures 4c–4f can be compared only qualitatively with time series reconstructed from ice cores [e.g., *Grootes et al.*, 1993] (Figure 2f), cave records [*Wang et al.*, 2001] (Figure 4a), and Chinese loess [*Sun et al.*, 2006] (Figure 4b). It is noteworthy that the summer precipitation in Eastern Asia (around 20°N–30°N, 90°E–140°E) was in a low phase during Heinrich events (Figure 2e), which is consistent with a relatively stronger westerly (Figures 4c and 4d) and a weaker AWM (Figure 4e) in northern winter as well as a weaker East Asian summer monsoon, the latter is evidenced by increased $\delta^{18}O$ of Hulu Cave stalagmites [*Wang et al.*, 2001] (Figure 4a). The stronger westerlies in northern winter over Eurasian continent can also be seen from the increased anomalies of u-component in the condition during a Heinrich event minus the warmest peak phase of a D/O cycle (Figure 5). The increased anomaly of westerlies has two centers located at 15°N and 45°N, respectively, over around 300 hPa (Figure 5). The model results depicted in Figure 6 reveal the differences of global distribution of sea level pressure and composite near-surface wind in northern winter, spring, and summer in condition during a Heinrich event minus the warmest phase of a D/O cycle. In Figures 6a and 6b, we can see that the Aleutian low is well developed (negative anomalies over the North Pacific) but the Icelandic low is relatively weakened (positive anomalies over the North Atlantic) during a Heinrich event than in a warm peak phase of a D/O cycle. This bimodel pattern of SLP is due to that the azonal component of SLP is computed using azonal component of sea level temperature, as described by *Petoukhov et al.* [2000, equation (17)]. Thus cooling over the North Atlantic associated with weakening of THC leads to positive SLP anomaly in this region and compensatory negative anomaly over the North Pacific. This result is very similar to CLIMBER-2 response to the shutdown of THC [*Ganopolski et al.*, 2001], as well as the result of coupled GCMs [e.g., *Manabe and Stouffer*, 2000; *Vellinga and Woods*, 2002; *Zhang and Delworth*, 2005]. The pattern in northern summer (Figure 6c) is almost the same as that in northern winter and spring but with a reduced south Atlantic and Indian High in the Southern Hemisphere. In East Asia an offshore surface wind component can be seen (Figure 6c),

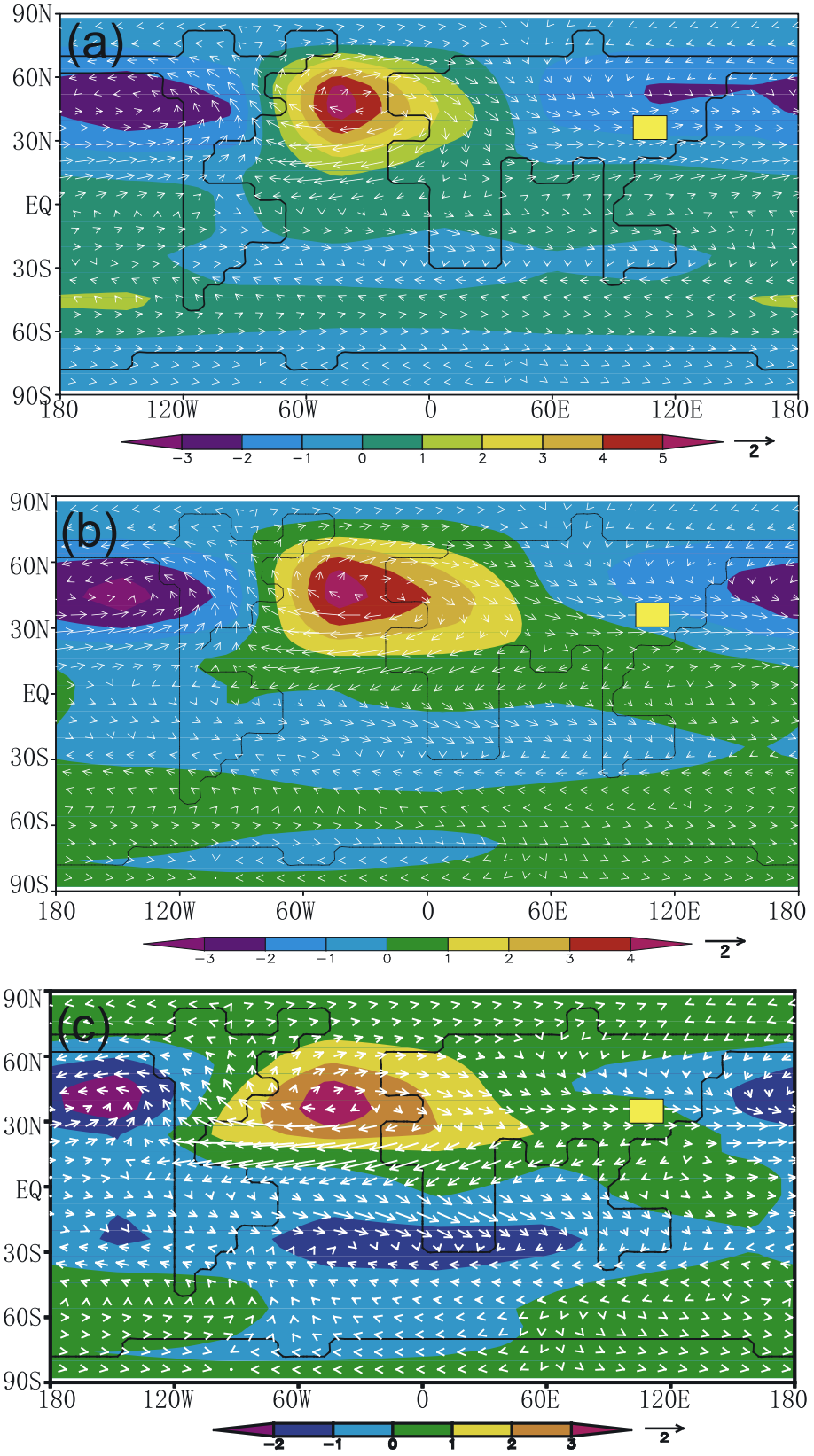

Figure 6. Global pattern of differences in model-simulated sea level surface pressure (unit: hPa) and mean near-surface wind (unit: m/s) in conditions during a Heinrich event minus the warmest phase of a D/O cycle. (a) Northern winter (DJF), (b) northern spring (MAM), and (c) northern summer (JJA).

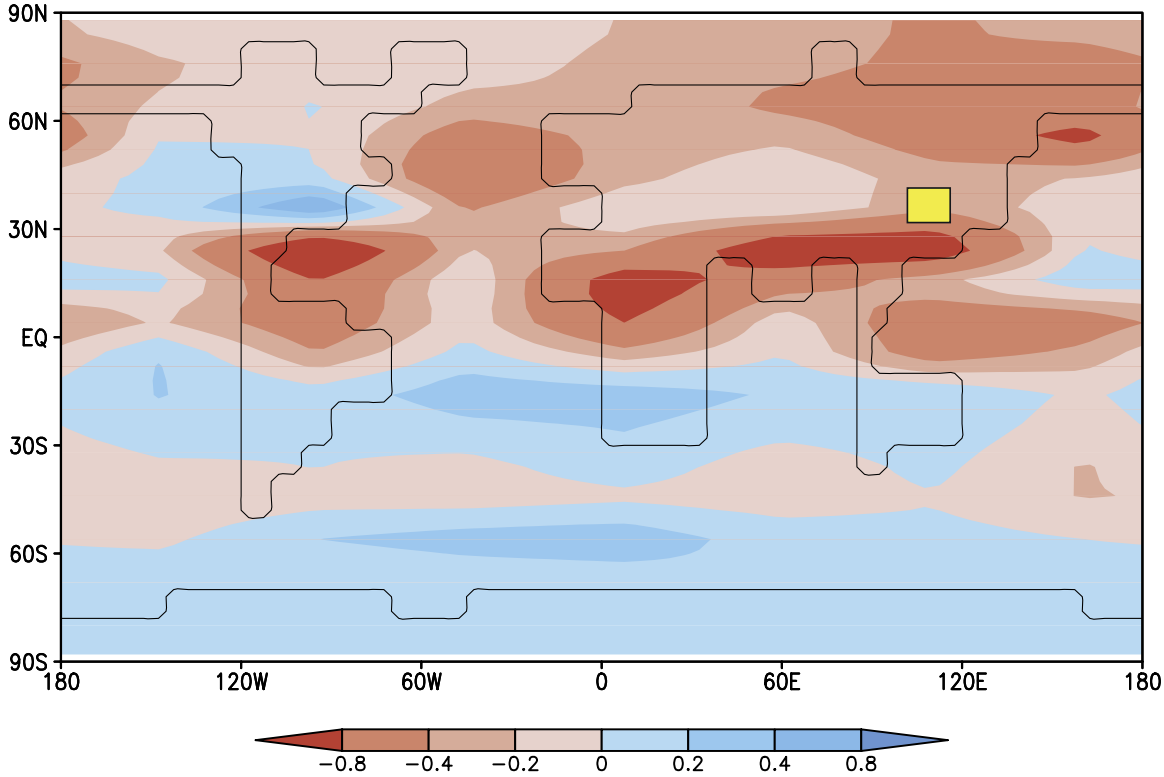

Figure 7. Global pattern of differences in model-simulated boreal summer precipitaion (unit: mm/day) in condition during a Heinrich event minus the warmest phase of a D/O cycle.

which indicates a weakening of summer monsoon associated with a decrease in summer precipitation during a Heinrich event than in a warm peak phase of a D/O cycle (Figure 7). Then the more arid conditions due to decreased summer precipitation can be developed with extend of dust source regions expanding to south toward the Loess Plateau.

4. Discussion and Conclusion

[21] Abundant paleoclimate evidence shows that millennial-scale climate variability is, in some way, related to North Atlantic Heinrich and D/O events in many regions of the world. We have used an Earth system model of intermediate complexity, CLIMBER-2, to theoretically study the response of East Asian climate to Heinrich events and a rapid transition to the warming phase (D/O events). To simulate Heinrich events, freshwater anomalies and anomalies in the Laurentide inland-ice mass were introduced in the model over the high northern Atlantic and North America, respectively. Small randomly varying freshwater anomalies over the high northern Atlantic were specified to trigger D/O events. D/O events were synchronized by some tiny 1500-year oscillations which in itself would be too weak to generate D/O events.

[22] It is to note here that previous works have shown that D/O events can be simulated in CLIMBER-2 model under a range of glacial conditions (i.e., climate must be considerably colder than the present one) by applying a weak freshwater forcing [*Ganopolski and Rahmstorf*, 2001a, 2001b, 2002; *Ganopolski*, 2003; *Claussen et al.*, 2003]. However, to simulate a realistic sequence of abrupt climate changes resembling the paleoclimate records, all components of forcings used in this paper are needed, which are the same as in the works of *Calov et al.* [2002] and *Ganopolski* [2003].

[23] A synchronous signal in the region of Eurasian continent has been found with respect to annual-mean near-surface air temperature variations in the northern North Atlantic in this experiment from CLIMBER-2. The linkage of climate in North Atlantic and Eurasia during glacial period was well recorded in the Chinese loess-paleosol sequences [*Porter and An*, 1995; *Guo et al.*, 1996; *Chen et al.*, 1997]. Generally, the atmospheric circulation regime over Asian continent is controlled by monsoon overlying westerly winds, which is responsible for the transportation and deposition of eolian material of northern China. So in previous studies of the Quaternary loess sections in the Chinese Loess Plateau, the grain size of loess records was usually considered as a proxy of winter Asian monsoon and its changes are commonly interpreted as having been controlled by changes in wind intensity [*An et al.*, 1991a, 1991b] and the loess-paleosol sequence be interpreted as indication of alternating waxings and wanings of the summer and winter Asian paleomonsoons where the soil-forming periods correspond to strengthened Asian summer monsoon and loess deposition correspond to strengthened Asian winter monsoon [*An et al.*, 1991a, 1991b; *Liu et al.*, 1995; *Maher et al.*, 1994]. However, this interpretation could be too oversimplified when compared to the observations, as *Ding et al.* [1999] strongly suggested that the spatial loess grain size changes of loess records seem to be controlled first by changes in the position of the deserts and

changes in the desert extent in northern China, which is closely related to the shifts in source areas of Asian dust that were synchronous with large-scale variations in atmospheric circulation [*Zhang et al.*, 1997]. Evidence from the high-resolution loess records suggests that two forcing mechanisms operate the behavior of climate changes in northern midlatitude during glacial time, of which one is the trend of global ice volume growing in the Northern Hemisphere, and the other is the forcing of D/O oscillations (i.e., Bond cycles) which superimposed on the first one [*Ren et al.*, 1996]. Sedimentary dynamic grain-size analysis has found that Chinese loess shows bimodal distribution composed of overlapped coarse and fine components, in which the coarse component was mostly controlled by the near-surface monsoonal circulation while the fine component was mainly transported by westerly winds in the last glacial-interglacial cycle in northern China [*Sun et al.*, 2003]. The modeling results show that during boreal winter, the strength of the westerlies in the midlatitudes of Eurasian continent gradually increased during the last glacial period (Figures 4c and 4d), especially during the Heinrich events, the westerlies reach maximum (Figures 4c and 4d). At the same time, the westerlies are relatively stronger during the Heinrich events than in the warmest peak phase of a D/O cycle in northern winter over Eurasian continent with two centers located at 15°N and 45°N, respectively, over 300 hPa (Figure 5). Our modeling results also reveal that over middle and eastern part of Eurasian continent, where the climate characteristics is mainly controlled by the Siberian High pressure cell in northern winter, the simulated sea level surface pressure was relatively weaker during Heinrich events than in the warmest phase of a D/O cycle (see negative anomaly of the sea level surface pressure in Figure 6a). However, as the changes of sea level surface pressure in this area are relatively small (see also the amplitude of the PI in Figure 4f) between stadials and interstadials, the modeling results do not necessarily confirm a substantial weakening of the Siberian High pressure and associated Asian winter monsoon. Contrast to the strengthened westerlies over Eurasian continent (40°E–140°E) during the Heinrich events, the model results reveal a decreased summer precipitation in south and southeast Asia including the Chinese Loess Plateau (Figure 7). As the Asian summer monsoon contributes most of the annual precipitation in this area, the decreased summer precipitation implies that the Asian summer monsoon is relatively weaker during the Heinrich events than in the warmest peak phase of a D/O cycle, which is also seen in Figure 6c that during northern summer, there is offshore wind along the south and east Asian coast. The simulated decreased summer rainfall is consistent with the decreased strength of the Asian summer monsoon inferred from the δ^{18}O of Hulu Cave stalagmites [*Wang et al.*, 2001]. The model results then imply that the northern China including the Chinese Loess Plateau was probably drier during Heinrich events due to the decreased summer rainfall and this increased aridity lead to expansion of the northern deserts. Our modeling results suggest that the relatively stronger westerlies from central Asia that entrain the bulk of Aeolian dust delivered to the Loess Plateau and more arid conditions in northern China due to weaker Asian summer monsoon during the Heinrich events are probably responsible for the Heinrich and D/O events-similar climate signals found in Chinese loess records during the last glaciation. However, because grain-size changes of loess deposits may be controlled not only by the extend of dust source regions, which can be influenced by regional arid conditions, and wind intensity (e.g., westerly wind or monsoon-induced wind), but also by other factors (e.g., postdepositional weathering) [*Ding et al.*, 1999], the mechanism of the similar climate signals both in Chinese loess records and in North Atlantic ice cores needs further investigation.

[24] In addition, although this modeling experiment has revealed some aspects of East Asian climate responding to the D/O and Heinrich events during the last glacial period, it is necessary to emphasize that owing to several limitations of our model (coarse spatial resolution, no changes in central Asian desert computed and a simplified description of atmospheric dynamics), the strength of atmospheric teleconnections is likely to be underestimated, so a comparison of the paleoproxy data with the model results should be considered as qualitative rather than quantitative. For example, the Hulu Cave δ^{18}O values have a large range (from −5 to −9‰) while model results (ZI, u, AWMI, and PI) have a relatively small range. It is important, however, that the sign and relative timing of simulated changes are fully consistent with paleoclimate data. Further experiments with higher spatial resolution climate model or coupled CLIMBER-2 with a regional climate model are expected to more precisely quantify climate changes in East Asia responding to the D/O and Heinrich events during the last glacial.

[25] **Acknowledgments.** This work was supported by the National Natural Science Foundation of China (NSFC) (grant 40571169), the NSFC Innovation Team Project (grant 40421101), and the research fund from the Key Laboratory of Arid Climatic Changing and Reducing Disaster of Gansu Province (grant IAM200406). The authors would like to thank three anonymous reviewers for their thoughtful comments and constructive suggestions on this paper. Jin L. is grateful to German Academic Exchange Service (DAAD) and China Scholarship Council (CSC) for providing him a scholarship during his research visit at Potsdam Institute for Climate Impact Research (PIK), Potsdam, Germany, whose hospitality is also appreciated.

References

Alley, R. B., S. Anandakrishnan, and P. Jung (2001), Stochastic resonance in the North Atlantic, *Paleoceanography*, *16*, 190–198.

An, Z. S., X. H. Wu, P. X. Wang, S. M. Wang, G. R. Dong, X. J. Sun, Y. C. Lu, S. L. Zhao, and S. H. Zheng (1991a), Paleomonsoon of China over the last 130 ka: I. Paleomonsoon records, *Sci. China, Ser. B.*, *34*, 1005–1015.

An, Z. S., X. H. Wu, P. X. Wang, S. M. Wang, G. R. Dong, X. J. Sun, Y. C. Lu, S. L. Zhao, and S. H. Zheng (1991b), Paleomonsoon of China over the last 130 ka: II. Paleomonsoon variation, *Sci. China, Ser. B*, *34*, 1016–1034.

An, Z. S., G. Kukla, S. C. Porter, and J. L. Xiao (1991c), Late Quaternary dust flow on the Chinese Loess Plateau, *Catena*, *18*, 125–132.

Berger, A. (1978), Long-term variations of daily insolation and quaternary climatic changes, *J. Atmos. Sci.*, *35*, 2362–2367.

Biscaye, P. E., F. E. Grousset, M. Revel, S. Van der Gaast, G. A. Zielinski, A. Vaars, and G. Kukla (1997), Asian provenance of last glacial maximum dust (stage 2) in the Greenland Ice Sheet Project 2 Ice Core, Summit, Greenland, *J. Geophys. Res.*, *102*, 26,765–26,782.

Bond, G., et al. (1992), Evidence for massive discharges of icebergs into the North Atlantic Ocean during the last glacial period, *Nature*, *360*, 245–249.

Bonnefille, R., F. Chalie, J. Guiot, and A. Vincens (1992), Quantitative estimates of full glacial temperatures in equatorial Africa from palynological data, *Clim. Dyn.*, *6*, 251–257.

Broecker, W. S. (1994), Massive iceberg discharges as triggers for global climate change, *Nature*, *372*, 421–424.

Broecker, W., G. Bond, K. Mieczyslawa, E. Clark, and J. McManus (1992), Origin of the northern Atlantic's Heinrich events, *Clim. Dyn.*, *6*, 265–273.

Brovkin, V., J. Bendtsen, M. Claussen, A. Ganopolski, C. Kubatzki, V. Petoukhov, and A. Andreev (2002), Carbon cycle, vegetation, and climate dynamics in the Holocene: Experiments with the CLIMBER-2 model, *Global Biogeochem. Cycles*, *16*(4), 1139, doi:10.1029/2001GB001662.

Calov, R., A. Ganopolski, V. Petoukhov, M. Claussen, and R. Greve (2002), Large-scale instabilities of the Laurentide ice sheet simulated in a fully coupled climate-system model, *Geophys. Res. Lett.*, *29*(24), 2216, doi:10.1029/2002GL016078.

Chen, F. H., J. Bloemendal, J. M. Wang, J. J. Li, and F. Oldfield (1997), High-resolution multi-proxy climate records from Chinese loess: Evidence for rapid climatic changes over the last 75 kyr, *Palaeogeogr. Palaeoclim. Palaeoecol.*, *130*, 323–335.

Chen, L. X., et al. (Eds.) (1991), *East Asian Monsoon* (in Chinese), 262 pp., China Meteorol. Press, Beijing.

Chen, W., H.-F. Graf, and R. Huang (1999), The interannual variability of East Asian winter monsoon and its relation to the summer monsoon, *Adv. Atmos. Sci.*, *17*, 48–60.

Claussen, M., A. Ganopolski, V. Brovkin, F.-W. Gerstengarbe, and P. Werner (2003), Simulated global-scale response of the climate system to Dansgaard/Oeschger and Heinrich events, *Clim. Dyn.*, *21*, 361–370.

Dansgaard, W., H. B. Claussen, N. Gundestrup, C. U. Hammer, S. F. Johnsen, P. M. Kristindottir, and N. Reeh (1982), A new Greenland deep ice core, *Science*, *218*, 1273–1277.

Dansgaard, W., et al. (1993), Evidence for general instability of past climate from a 250-kyr ice-core record, *Nature*, *364*, 218–220.

de Garidel-Thoron, T., L. Beaufort, B. K. Linsley, and S. Dannenmann (2001), Millennial-scale dynamics of the East Asian winter monsoon during the last 200,000 years, *Paleoceanography*, *16*, 491–502.

Denton, G. H., R. B. Alley, G. C. Comer, and W. S. Broecker (2005), The role of seasonality in abrupt climate change, *Quat. Sci. Rev.*, *24*, 1159–1182.

Ding, Z. L., N. W. Rutter, J. T. Han, and T. Liu (1992), A coupled environmental system formed at about 2.5 Ma B.P in East Asia, *Palaeogeogr. Palaeoclim. Palaeoecol.*, *94*, 223–242.

Ding, Z., Z. Yu, N. W. Rutter, and T. Liu (1994), Towards an orbital time scale for Chinese loess deposits, *Quat. Sci. Rev.*, *13*, 39–70.

Ding, Z., J. Sun, and D. Liu (1999), A sedimentological proxy indicator linking changes in loess and deserts in the Quaternary, *Sci. China, Ser. D.*, *42*, 146–152.

Dong, G. R., J. Jin, and S. Y. Gao (1990), Climatic changes since the late Pleistocene in deserts of northern China, *Quat. Sci.*, *3*, 213–222. (In Chinese with English abstract.)

Elliot, M., L. Labeyrie, and J.-C. Duplessy (2002), Changes in North Atlantic deep-water formation associated with the Dansgaard-Oeschger temperature oscillations (60–10 ka), *Quat. Sci. Rev.*, *21*, 1153–1165.

Ganopolski, A. (2003), Glacial integrative modeling, *Philos. Trans. R. Soc., Ser. A.*, *361*, 1871–1884.

Ganopolski, A., and S. Rahmstorf (2001a), Rapid changes of glacial climate simulated in a coupled climate model, *Nature*, *409*, 153–158.

Ganopolski, A., and S. Rahmstorf (2001b), Stability and variability of the thermohaline circulation in the past and future: A study with a coupled model of intermediate complexity, in *The Oceans and Rapid Climate Change: Past, Present and Future*, edited by D. Seidov et al., pp. 261–275, AGU, Washington, D. C.

Ganopolski, A., and S. Rahmstorf (2002), Abrupt glacial climate changes due to stochastic resonance, *Phys. Rev. Lett.*, *88*, 038501, doi:10.1103/PhysRevLett.88.038501.

Ganopolski, A., S. Rahmstorf, V. Petoukhov, and M. Claussen (1998), Simulation of modern and glacial climates with a coupled model of intermediate complexity, *Nature*, *391*, 351–356.

Ganopolski, A., V. Petoukhov, S. Rahmstorf, V. Brovkin, M. Claussen, A. Eliseev, and C. Kubatzki (2001), CLIMBER-2: A climate system model of intermediate complexity. Part II: Model sensitivity, *Clim. Dyn.*, *17*, 735–751.

Grimm, E. C., G. L. Jacobson Jr., W. A. Watts, B. C. S. Hansen, and K. A. Maasch (1993), A 50,000-year record of climate oscillations from Florida and its temporal correlation with the Heinrich events, *Science*, *261*, 198–200.

Grootes, P. M., M. Stulver, J. W. C. White, S. Johnsen, and J. Jouzel (1993), Comparison of oxygen isotope records from GISP2 and GRIP Greenland ice cores, *Nature*, *366*, 552–554.

Guiot, J., A. Pons, J. L. de Beaulieu, and M. Reille (1989), A 140,000-year continental climate reconstruction from two European pollen records, *Nature*, *338*, 309–313.

Guiot, J., D. J. L. Beaulieu, R. Cheddadi, F. David, P. Ponel, and M. Reille (1993), The climate in western Europe during the last Glacial/Interglacial cycle derived from pollen and insect remains, *Palaeogeogr. Palaeoclim. Palaeoecol.*, *103*, 73–93.

Guo, Z., T. Liu, J. Guiot, N. Wu, H. Lü, J. Liu, and Z. Gu (1996), High frequency pulses of East Asian monsoon climate in the last two glaciations: Link with the North Atlantic, *Clim. Dyn.*, *12*, 701–709.

Guo, Z., P. Biscaye, L. Wei, X. Chen, S. Peng, and T. Liu (2000), Summer monsoon variations over the last 1.2 Ma from the weathering of loess-soil sequences in China, *Geophys. Res. Lett.*, *27*, 1751–1754.

Heinrich, H. (1988), Origin and consequences of cyclic ice rafting in the northeast Atlantic Ocean during the past 130,000 years, *Quat. Res.*, *29*, 142–152.

Hu, Z. Z., L. Bengtsson, and K. Arpe (2000), Impact of global warming on the Asian winter monsoon in a coupled GCM, *J. Geophys. Res.*, *105*, 4607–4624.

Ji, L., S. Sun, K. Arpe, and L. Bengtsson (1997), Model study on the interannual variability of Asian winter monsoon and its influence, *Adv. Atmos. Sci.*, *14*, 1–22.

Jin, L., A. Ganopolski, F. Chen, M. Claussen, and H. Wang (2005), Impacts of snow and glaciers over Tibetan Plateau on Holocene climate change: Sensitivity experiments with a coupled model of intermediate complexity, *Geophys. Res. Lett.*, *32*, L17709, doi:10.1029/2005GL023202.

Kukla, G., and Z. S. An (1989), Loess stratigraphy in central China, *Palaeogeogr. Palaeoclim. Palaeoecol.*, *72*, 203–225.

Kutzbach, J. E., P. J. Guetter, P. J. Behling, and R. Selin (1993), Simulated climatic changes: results of the COHMAP climate-model experiments, in *Global Climates Since the Last Glacial Maximum*, edited by H. E. Wright Jr. et al., pp. 24–93, Univ. of Minnesota Press, Minneapolis.

Landais, A., J. Jouzel, V. Masson-Delmotte, and N. Caillon (2005), Large temperature variations over rapid climatic events in Greenland: A method based on air isotopic measurements, *C. R. Geosci.*, *337*, 947–956.

Linsley, B. K. (1996), Oxygen-isotope record of sea-level and climate variations in the Sulu Sea over the past 150,000 years, *Nature*, *380*, 234–237.

Lowell, T. V., C. J. Heussser, B. G. Andersen, P. I. Moreno, A. Hauser, L. E. Heusser, C. Schluchter, D. R. Marchant, and G. H. Genton (1995), Interhemispheric correlation of late Pleistocene glacial events, *Science*, *269*, 1541–1549.

Liu, T. S., (Ed.) (1985), *Loess and Environment*, 251 pp., China Ocean Press, Beijing.

Liu, T. S., Z. T. Guo, J. Q. Liu, J. M. Han, Z. L. Ding, Z. Y. Gu, and N. Q. Wu (1995), Variations of eastern Asian monsoon over the last 140,000 years, *Bull. Soc. Géol. Fr.*, *166*, 221–229.

Lü, H. Y., Y. J. Wang, J. Q. Wu, and J. Wang (1991), Preliminary study on the relationship between century-long climatic fluctuations and celestial body movements during the recent 20 ka BP in China, in *Quaternary Land-Sea Correlation in China*, edited by M. S. Liang and J. L. Zhang, pp. 173–187, Science Press, Beijing.

Maher, B. A., R. Thompson, and L. P. Zhou (1994), Spatial and temporal reconstruction of changes in the Asian paleomonsoon: A new mineral magnetic approach, *Earth Planet. Sci. Lett.*, *125*, 461–471.

Manabe, S., and R. J. Stouffer (1988), Two stable equilibria of a coupled ocean-atmosphere model, *J. Clim.*, *1*, 841–866.

Manabe, S., and R. J. Stouffer (2000), Study of abrupt climate change by a coupled ocean-atmosphere model, *Quat. Sci. Rev.*, *19*, 285–299.

Peixoto, J., and A. Oort (1992), *Physics of Climate*, 520 pp., Am. Inst. Phys., New York.

Petit, J. R., et al. (1999), Climate and atmospheric history of the past 420,000 years from Vostol ice core, Antactica, *Nature*, *399*, 429–436.

Petoukhov, V., A. Ganopolski, V. Brovkin, M. Claussen, A. Eliseev, C. Kubatzki, and S. Rahmstorf (2000), CLIMBER-2: A climate system model of intermediate complexity. Part I: Model description and performance for present climate, *Clim. Dyn.*, *16*, 1–17.

Porter, S. C. (2001), Chinese loess record of monsoon climate during the last glacial-interglacial cycle, *Earth Sci. Rev.*, *54*, 115–128.

Porter, S. C., and Z. S. An (1995), Correlation between climate events in the Northern Atlantic and China during the last glacial, *Nature*, *375*, 305–308.

Ren, J., Z. Ding, T. Liu, J. Sun, and X. Zhou (1996), Climatic changes on millennial time scales–Evidence from a high-resolution loess record, *Sci. China, Ser. D.*, *39*, 449–459.

Rind, D., D. Peteet, A. Mclntyre, and W. Ruddiman (1986), The impact of cold North Atlantic sea surface temperatures on climate: Implications for the Younger Dryas cooling (11–10 k), *Clim. Dyn.*, *1*, 3–33.

Rossby, C. G. (1939), Relationship between variations in the intensity of the zonal variation and displacement of the semi-permanent centers of action, *J. Mar. Res.*, *2*, 38–55.

Stocker, T. F., D. G. Wright, and L. A. Mysak (1992), A zonally averaged, coupled ocean-atmosphere model for paleoclimate studies, *J. Clim.*, *5*, 773–797.

Sun, D., Z. An, R. Su, H. Lu, and Y. Sun (2003), Eolian sedimentary records for the evolution of monsoon and westerly circulations of northern China in the last 2.6 Ma, *Sci. China, Ser. D.*, *46*, 1049–1059.

Sun, Y., S. C. Clemens, Z. An, and Z. Yu (2006), Astronomical timescale and palaeoclimatic implication of stacked 3.6-Myr monsoon records from the Chinese Loess Plateau, *Quat. Sci. Rev.*, *25*, 33–48.

Vellinga, M., and R. A. Woods (2002), Global climatic impacts of a collapse of the Atlantic thermohaline circulation, *Clim. Change*, *54*, 251–267.

Verosub, K. L., P. Fine, M. J. Singer, and J. TenPas (1993), Pedogenesis and paleoclimate: Interpretation of the magnetic susceptibility record of Chinese loess-paleosol sequences, *Geology*, *21*, 1011–1014.

Vincens, A., F. Chakie, and R. Bonnefille (1993), Pollen-derived rainfall and temperature estimates from Lake Tanganyika and their implication for Late Pleistocene water levels, *Quat. Rev.*, *40*, 343–350.

Voelker, A. H. L., and workshop participants (2002), Global distribution of centennial-scale records for marine isotope stage (MIS) 3: A database, *Quat. Sci. Rev.*, *21*, 1185–1212.

Wang, Y. J., H. Cheng, R. L. Edwards, Z. S. An, J. Y. Wu, C.-C. Shen, and J. A. Dorale (2001), A high-resolution absolute-dated late Pleistocene monsoon record from Hulu Cave, China, *Science*, *294*, 2345–2348.

Xiao, J. L., S. C. Porter, Z. S. An, H. Kumai, and S. Yoshikawa (1995), Grain size of quartz as an indicator of winter monsoon strength on the Loess Plateau of central China during the last 130,000 yr., *Quat. Res.*, *43*, 22–29.

Zhang, R., and T. L. Delworth (2005), Simulated tropical response to a substantial weakening of the Atlantic thermohaline circulation, *J. Clim.*, *18*, 1853–1860.

Zhang, X. Y., R. Arimoto, and Z. S. An (1997), Dust emission from Chinese desert sources linked to variations in atmospheric circulation, *J. Geophys. Res.*, *102*, 28,041–28,044.

F. Chen and L. Jin, Key Laboratory of Western China's Environmental Systems (Ministry of Education) and Key Laboratory of Arid Climatic Changing and Reducing Disaster of Gansu Province, Lanzhou University, South Tianshui Road 222, Lanzhou 730000, China. (fhchen@lzu.edu.cn)

M. Claussen, Meteorological Institute, University Hamburg and Max Planck Institute for Meteorology, Bundesstr. 53, D-20146 Hamburg, Germany. (martin.claussen@zmaw.de)

A. Ganopolski, Potsdam Institute for Climate Impact Research, P. O. Box 601203, D-14412 Potsdam, Germany. (andrey@pik-potsdam.de)